

Tarzan: Passively-Learned Real-Time Rate Control for Video Conferencing

Neil Agarwal[¶] Rui Pan[¶] Francis Y. Yan[†] Ravi Netravali[¶]

[¶]Princeton University [†]Microsoft Research and UIUC

Abstract

Rate control algorithms are at the heart of video conferencing platforms, determining target bitrates that match dynamic network characteristics for high quality. Recent data-driven strategies have shown promise for this challenging task, but the performance degradation they introduce during training has been a nonstarter for many production services, precluding adoption. This paper aims to bolster the *practicality* of data-driven rate control by presenting an alternative avenue for experiential learning: leveraging purely existing telemetry logs produced by the incumbent algorithm in production. We observe that these logs often contain effective decisions, although often at the wrong times or in the wrong order. To realize this approach despite the inherent uncertainty that log-based learning brings (i.e., lack of feedback for new decisions), our system, Tarzan, combines a variety of robust learning techniques (i.e., conservatively reasoning about alternate behavior to minimize risk and using a richer model formulation to account for environmental noise). Across diverse networks (emulated and real-world), Tarzan outperforms the widely deployed GCC algorithm, increasing average video bitrates by 15–39% while reducing freeze rates by 60–100%.

1 INTRODUCTION

Real-time video conferencing is integral to our daily lives, with widespread use cases across many societal pathways including healthcare, education, gaming, and more. Key to their functionality are the rate control algorithms (e.g., Google Congestion Control or GCC [17]) that conferencing platforms employ. These algorithms are tasked with quickly (e.g., every 50 ms) characterizing network performance based on recent transmissions and selecting a target bitrate for the upcoming frames that maximizes content quality without introducing undue latency or stalls. This value is then shared with the local video codec which performs best-effort compression of the raw frames to match the target prior to transmission.

Recent years have witnessed a flurry of proposals for improving conferencing quality via improved rate control. Most notably, numerous data-driven approaches have shown how reinforcement learning (RL)-based algorithms can substantially outperform GCC’s hand-tuned variants [47–49]. As in

other networked-system domains [14, 29, 44, 45], the key is in making better use of dense application- and network-layer feedback signals to enable bitrate changes that more closely track rapid network fluctuations in the wild—a key challenge for GCC [17, 47–49].

Yet, despite their promise, data-driven rate control algorithms have seen minimal adoption in practice. Our conversations with operators of large-scale conference platforms reveal that the primary showstopper is the impact that these schemes have on the performance or quality of experience (QoE) observed by real users. Indeed, the experiential learning that these schemes pursue *in real conferencing sessions* fundamentally involves exploring different rate decisions—both good and bad for QoE—and observing their effects in certain scenarios. Our experiments show that this trial-and-error process can increase video freeze rates up to 79% and degrade video bitrates by up to 77%, yielding unacceptable QoE (§2.2). Data-driven strategies could forego such user-facing training by relying on simulators and emulators, but this may jeopardize efficacy in production settings due to the “simulation to reality” gap [12, 16, 22, 44, 48].

This paper aims to build on recent data-driven rate control schemes, not by designing more performant algorithms, but instead by *bolstering their practicality*. Our key insight is that the fine-grained telemetry logs that production conferencing platforms routinely capture for debugging and retrospective optimization [1, 2, 4, 7, 10] already embed sufficient insight to guide data-driven algorithms to outperform their hand-tuned counterparts. The reason is that, while algorithms like GCC struggle to quickly match fluctuating network bandwidths, they often adjust target rates in the appropriate direction with delay (Figure 1). Consequently, we find that simply reorganizing the same decisions that GCC makes during video sessions (without exploring any alternate rate values) boosts conferencing bitrates by 19% and decreases freezes by 80% (§3.3).

We present **Tarzan**, an end-to-end system that realizes such log-based learning to practically enhance rate control in video conferencing. Tarzan starts by representing production telemetry logs that reflect the behavior and performance of a deployed algorithm (e.g., GCC) as more traditional (state, action, reward) tuples for RL. These logs then guide Tarzan’s

experiential learning, which follows the soft actor-critic algorithm [25] to develop a lightweight neural network for rate control. Training occurs entirely offline using only logs (i.e., no video playback or simulation), and the resultant model is shipped to clients for deployment.

Though conceptually straightforward, learning in this offline manner faces several challenges centered around *uncertainty* (§3.4). As noted above, the feasible learned improvements are rooted in discovering alternate sequences of logged actions that perform better in certain scenarios. However, assessing such sequences is fundamentally risky as they involve applying previously-seen actions to new scenarios without guarantees that the benefits will port, i.e., unlike traditional RL, we lack direct feedback for these new sequences. This limitation is worsened by the fact that logs in conferencing systems (1) typically reflect singular deterministic policies with little variation in action for a given scenario, and (2) are inherently noisy in that observed performance can be influenced not only by rate decisions, but also external phenomena such as codec behavior and stochastic network variations [23, 43, 44, 46, 49].

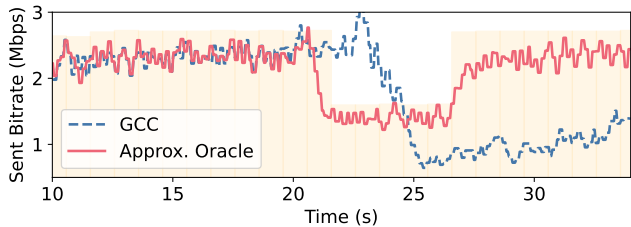
To manage uncertainty, Tarzan incorporates two key techniques. First, when estimating the consequence of an action in a given scenario, Tarzan takes a *conservative* approach—it lowers the estimated return if no similar state-action pair has been observed before, and proceeds only when the performance improvement outweighs the risk. Second, rather than estimating a single expected outcome, Tarzan explicitly tackles environmental variance by learning a *distribution* over all possible outcomes. This distributional perspective provides Tarzan with richer insights, enabling more informed decision-making. We detail the concrete algorithms in §4.2.

We evaluated Tarzan on a diverse set of emulated and real-world networks spanning 3G–5G cellular and wired broadband links. Overall, we observe that Tarzan consistently outperforms GCC, increasing average video bitrates by 15–39% while reducing freeze rates by 60–100%. Further, Tarzan’s wins closely mimic those of recent (impractical) online RL algorithms [22, 47, 48], falling within 0.5–13.1% and 0–19% for average bitrates and freeze rates, respectively.

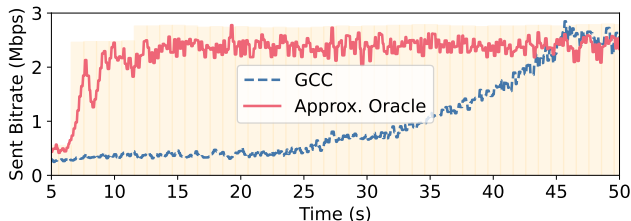
2 BACKGROUND & MOTIVATION

2.1 Prior Work

Rule-based heuristics. Today’s video conferencing applications (e.g., Microsoft Teams, Google Hangouts, Zoom) rely on rule-based algorithms to provide network bandwidth estimates and guidance as to how to tune the encoding and sending bitrates over time. A widely used, publicly available algorithm is Google Congestion Control (GCC) [17]. GCC first characterizes the current network usage based on recent packet delay and loss measurements, and then updates the target bitrate according to a fixed set of rules (e.g., when the observed packet loss is less than 2%, increase the target bitrate



(a) GCC overshoots network capacity after a bandwidth drop, causing video freezes.



(b) After an intermittent bandwidth drop, GCC ramps up slowly, leading to suboptimal bandwidth utilization.

Figure 1: Examples of GCC’s pitfalls, which occur primarily in dynamic network conditions. To illustrate potential performance improvement opportunities, we plot the behavior of an oracle algorithm.

by 5%, or when the system is in a “decrease” state, reduce the target bitrate by 15%).

Google Congestion Control (and other rule-based heuristics) have been widely observed to be suboptimal [22, 23, 47–49]. Recent reports have found that when using state-of-the-art rule-based heuristics, over 20% of over a million video conferencing sessions experience poor performance [49]. Digging deeper, we find that GCC performs particularly poorly in highly dynamic network conditions, where the available bandwidth fluctuates (e.g., in cellular networks). The general hardcoded set of rules fails to fully leverage the dense signals from the application and network that are necessary for predicting the appropriate corresponding bitrate adjustments in these highly variable regimes.

As a result, for example, when bandwidth drops, GCC can fail to rapidly and appropriately adjust the bandwidth, unnecessarily overshooting the available network capacity and incurring video freezes for users (Fig. 1a). Further, after an intermittent drop in bandwidth, GCC can be unnecessarily delayed in fully ramping up to the available bandwidth (Fig. 1b). As quality expectations for video conferencing steadily increase with its growing ubiquity, there is a pressing need to find improved rate control algorithms over today’s rule-based heuristics.

Data-driven approaches. In response, the community has explored the use of data-driven approaches to generate alternative rate control algorithms (e.g., R3Net [22], OnRL [48], Loki [47]). Such machine learning-based approaches are

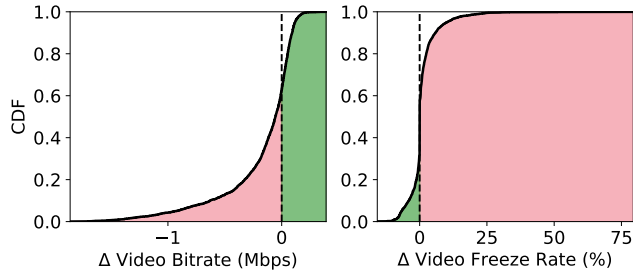


Figure 2: Distribution of changes to video QoE observed (relative to GCC) for video conferencing sessions during online RL model training. Improvements are shaded in green; degradations are shaded in red.

particularly skilled at extracting patterns from highly-dense information and have been shown to deliver nontrivial improvements over today’s state-of-the-art rule-based heuristics. Given the challenge of explicitly identifying the exact action an algorithm should take in each scenario and using standard supervised learning techniques to learn that mapping, recent proposals have opted to leverage reinforcement learning (RL). An RL agent learns by interacting with the environment and leveraging feedback from the environment to iteratively adjust its behavior to maximize cumulative reward over a horizon. In the case of rate control for video conferencing, the RL agent outputs bitrate updates and leverages the transport/application layer feedback to update its decision-making policy.

2.2 Motivations

As confirmed by prior work [22, 47, 48] and our results in §5, data-driven methods can deliver significant wins over rule-based heuristics and are crucial to enabling the effective rate control that today’s video conferencing applications demand. Surprisingly, despite their potential benefits, these solutions have yet to gain traction in production deployments. In conversations with the operators of major production video conferencing deployments, these solutions do not meet the practicality constraints of production environments. In particular, the biggest concern is the disruption of client video conferencing sessions during model training.

Fundamental to existing solutions is their use of reinforcement learning, a trial-and-error learning mechanism that trains a model by iteratively interacting with an environment and updating the model based on the interaction outcomes. For existing solutions, randomly initialized RL agents (models) are placed directly on client devices and are allowed to dictate the bitrate decisions for real user-facing video conferencing sessions. Over time, the models gain experience and converge to a high-performing policy; however, this comes at the cost of disruption to the quality of video conferencing calls during the training process. Prior approaches explicitly encourage exploration of different actions and behavior during training (by adding an entropy bonus to the learning objective); the bitrate decisions taken during exploration may be far from the ideal

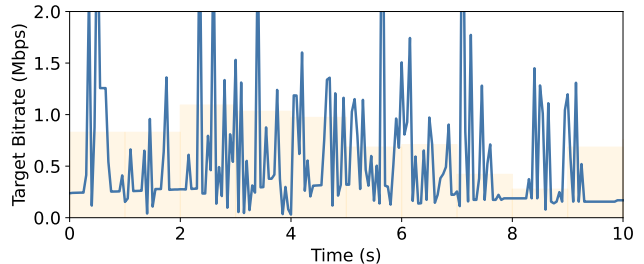


Figure 3: Example disruptive behavior observed during training of an online RL model; ground-truth network bandwidth is shaded in yellow.

bitrate decision for that particular scenario and dramatically degrade the quality of a video call.

To observe how the performance of video conferencing sessions is affected during training, we ran a series of experiments. We train an online RL algorithm in our video conferencing testbed and periodically record the QoE metrics of affected sessions. More details about our video conferencing testbed, online RL implementation, and QoE metrics can be found in §5. Note that our implementation includes the temporary fallback mechanism introduced by OnRL [48] which switches back to the rule-based heuristic when overuse is detected in the hope of reducing catastrophic behavior.

Fig. 2 shows the effects on performance (relative to GCC) during model training for two key QoE metrics. We find that 62% of calls experience a worse average video bitrate, with degradations as low as -1.9 Mbps (for context, the average bitrate of a call is 1.03 Mbps). 43% of calls experience higher video freeze rates, with freeze rate increases as much as +79%. Intuitively, these performance degradations are due to the exploratory nature of online RL mechanisms. Figure 3 highlights some of the disruptive behavior that causes performance degradations: repeated switching between low and high bitrates, bandwidth underutilization, and overaggressive bitrate ramp-ups. Fallback mechanisms fail to resolve these issues because they are only activated once catastrophic behavior is detected. Further, these degradations are exacerbated by the iterative development process of model optimization across different model designs and hyperparameters—the costs of training (e.g., QoE degradations) will be incurred every time.

Alternatively, prior work (e.g., R3Net [22], OnRL [48], Concerto [49]) has explored training models in simulation or preproduction deployments to avoid degrading video conferencing quality for existing clients. However, the trained models have been shown to perform inadequately upon deployment; the reason is that these alternative environments fail to capture the dynamics of production environments in full fidelity and any slight deviation of the environment can cause cascading effects on performance. In the literature, this performance gap is referred to as the “simulation to reality gap” [12, 16].

Work in other networked domains (e.g., Sage [45] for TCP

congestion control) learns from logs in an offline manner. However, this work requires running and collecting data for dozens of different existing congestion control algorithms; in contrast, the logs of production conferencing systems typically only include the experiences of a single rate control algorithm (e.g., GCC).

Summary. Recent data-driven approaches demonstrate considerable improvements over their rule-based counterparts. However, they face minimal adoption in production systems due to the disruptive nature of their interactive trial-and-error-based online learning approach. Alternatively, data-driven algorithms trained in simulations perform poorly when deployed to real production systems due to the “simulation to reality” gap. How to capitalize on the performance improvements offered by data-driven approaches while adhering to the constraints of production environments is an open question faced by video conferencing system operators.

3 VISION: LEARNING BY OBSERVATION

In this paper, we claim that there is a viable path forward, but it requires rethinking the end-to-end design of data-driven rate control systems, from how we source the data to how we leverage and learn from it.

3.1 The Data of Prior Approaches

Prior data-driven approaches collect training data by iteratively deploying and continually updating DNN-based rate control policies in production video conferencing systems, and logging the resulting behavior and outcomes [22, 47, 48]. These logs are shipped from users to a central server, where they are processed and then fed to a training algorithm that updates the weights underlying the current version of the rate control policy. The updated weights are shipped out to the clients and the next round of training proceeds.

At the central server, data processing of the logs involves extracting structured sequential data, i.e., series of (state, action, reward) tuples. A (s_t, a_t, r_t) tuple represents the following: at a given time t , the rate control policy takes as input recently observed information about application and transport layers (captured as vector s_t) and outputs an updated target bitrate a_t . The effect of updating the target bitrate to a_t on application performance (e.g., the change in video throughput, freezes, frame delay, etc.) is quantified as r_t . Such sequences of (state, action, reward) tuples offer a structured way to reflect the experiences and effects of a rate control policy.

This data provides critical feedback to the training process by reinforcing decision-making that leads to good behavior (high reward) and penalizing decision-making that leads to poor behavior (low reward). Recall that the training algorithm initially knows nothing about the environment or the ideal behavior. As a result, the initial rate control policies take random actions. This exploratory behavior helps build a growing set of diverse experiences, each trajectory corresponding to a different sequence of possible decisions. Over time, as the

weights of the rate control policies are updated and additional logs are collected, the model identifies high-potential paths and ultimately, converges to a policy that maximizes the cumulative reward. In the process, each step of deployment and data collection provides a critical feedback loop, enabling the training algorithm to (1) try and test out new behaviors, and (2) correct any misunderstandings about expected behavior in the learned model.

However, as quantified in §2.2, accumulating this rich and diverse dataset requires deploying partially trained policies to production environments and disrupting the quality of video conferencing sessions for users. From the perspective of a production deployment operator, this is not a viable option.

3.2 An Alternative Source of Data

In this paper, we posit that there is a viable alternative source of data—the experiences of the rule-based algorithm *currently deployed* in production settings for rate control (e.g., Google Congestion Control). Unlike the data of prior approaches, this source of data can be acquired without deploying partially trained or untested rate control policies and incurring the disruption described in §2.2. Instead, it is collected from a rate control heuristic already deployed in production at a fine granularity for the purposes of monitoring, debugging, and improving the heuristic algorithm [2, 6]. They can be prepared in a similar way to the post-processing of logs in prior approaches to extract sequences of (state, action, reward) tuples that reflect the experiences of the deployed rate control policy.

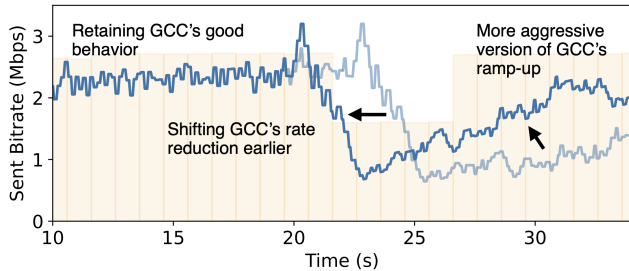
However, ultimately, these logs reflect the behavior of a single, static rate control policy (the in-house rule-based heuristic, e.g., GCC). The logs of prior approaches, on the other hand, reflect the behavior of hundreds of rate control policies, learned and deployed over hundreds of epochs of training. As previously described, the diversity in behaviors enables the algorithm to learn an effective rate control policy. This begs the question: how we can learn a better rate control policy from the experiences of a single rate control policy?

Besides the interactive reinforcement learning approaches of prior work, there exist alternative data-driven approaches such as imitation learning (e.g., behavior cloning) [26]. However, the goal of these methods is to learn the *same* behavior as reflected in the training data; our goal is to learn a *better* rate control strategy.

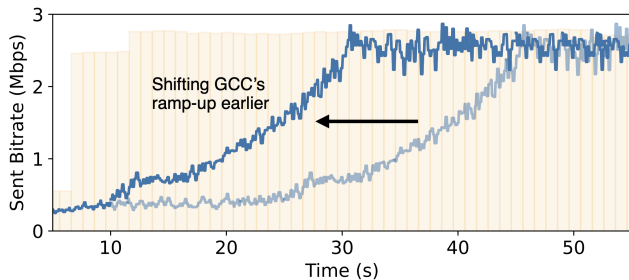
3.3 Opportunity

In this section, we introduce a novel approach to learning from the logs of GCC; we start by describing a key observation about the nature of GCC’s shortcomings.

As described in §2.1, GCC performs poorly in network traces with high bandwidth dynamism, resulting in either underutilization or overutilization of available network capacity. However, we observe GCC’s shortcomings are not due to a lack of adaptation but rather a delay in doing so. For example, in Fig. 4a, after the available bandwidth drops at $t=22$, it takes



(a) After the network bandwidth drops at $t=22$, it takes 3 seconds for GCC’s sending bitrate to catch up. By shifting GCC’s bitrate reduction earlier, we can reduce the degree of network overutilization, thereby decreasing the duration of video freezes.



(b) After the network bandwidth increases at $t=7$, it takes 40 seconds for GCC’s sending bitrate to catch up. By shifting GCC’s bitrate ramp-up earlier, we can increase network utilization, delivering increased video bitrates.

Figure 4: Potential improvements by rearranging sequences of actions within GCC’s logs; the network traces featured are the same as in Fig. 1.

3 seconds for GCC’s bitrate to catch up. Subsequently, GCC increases the target bitrate but is overly conservative in doing so. In Fig. 4b, after the available bandwidth increases, it takes 40 seconds for GCC’s bitrate to ramp up. In both of these cases, GCC adjusts the target rate in the appropriate direction.

This observation presents a unique learning opportunity: if similar network conditions were to be seen again, an algorithm could potentially do better than GCC by shifting GCC’s adaptation steps earlier. For example, in Fig. 4a, we can decrease freeze rates by shifting GCC’s bitrate reduction earlier and further increase the video bitrate by slightly increasing the rate of GCC’s ramp up. In Fig. 4b, we can improve upon GCC by ramping up sooner. Both of these examples demonstrate how reorganizing the actions (and sequences of actions) observed in existing GCC logs can potentially deliver improvements over GCC.

To quantify the potential benefits of this approach, we implemented an approximate oracle algorithm (i.e., it has access to ground-truth network dynamics) that using only actions observed within a given GCC log, identifies the optimal sequence of target bitrate updates. Applying this oracle algorithm to the network trace featured in Fig. 4a leads to a 52% increase in video bitrate and a 98% decrease in video freeze

rates; video bitrates increase by 80% and video freeze rates decrease by 79% in Fig. 4b. Across our entire corpus of network traces (more details in §5), this algorithm achieves a 19% increase in video bitrate and an 80% decrease in video freeze rate over GCC.

3.4 Challenges

However, realizing this approach in a way that is both practical and effective while adhering to the constraints of a production deployment setting requires addressing two key challenges.

Challenge #1: Lack of feedback. Ultimately, the goal is to learn an improved rate control policy without disrupting users (the main pitfall of prior approaches). However, producing an improved rate control policy requires learning a strategy that deviates from the behavior seen in the GCC logs (e.g., an alternative sequence of actions). Learning this alternative (and better) strategy requires reasoning about (and extrapolating) the expected outcomes of alternative behaviors. This is a risky proposition without access to feedback (i.e., testing the new strategy and validating the prediction). The greater the deviation, the greater the potential risk of extrapolation error; any errors in extrapolating will compound, as the resulting deviation will lead to more deviation. Ultimately, this comes at the detriment of the performance of the learned policy. In the field of learning sequential decision-making without feedback, this phenomenon is referred to as “distribution shift” [28]. In our evaluation ablation studies (§5.5), we find that failing to address distribution shift can dramatically cause performance degradations, increasing P90 video freeze rates over $12\times$. To address this issue in the context of learning improved rate control policies, we need a way to effectively balance decision-making deviations with risk mitigation.

Challenge #2: Environmental variance. Further complicating the ability to develop an understanding of how any given target bitrate update affects observed outcomes (rewards) is the presence of external phenomena outside the control of the bitrate decision-making policy that affect application behavior and ultimately, the outcomes of a given bitrate update. Unlike prior work [22, 49] that leverages emulation or simulation-based systems and can control for (or eliminate) the amount of noise introduced, production-based deployments do not have that luxury. Concretely, we find that this noise manifests in two ways. First, video conferencing applications apply additional downstream application logic after consuming a target bitrate update from the bitrate controller; this logic affects the *achieved* encoding and sending bitrate [23, 49]. Second, network conditions change rapidly (often in unpredictable ways [43, 44, 46])—taking the same action at the same state in two different instances could result in different outcomes because of rapid changes in network conditions (i.e., the bandwidth dropped). Ultimately, this makes it challenging to tell whether the observed outcome of two bitrate decisions differs due to external processes or the quality of the target bitrate decision. In our evaluation studies (§5.5), we find that failing

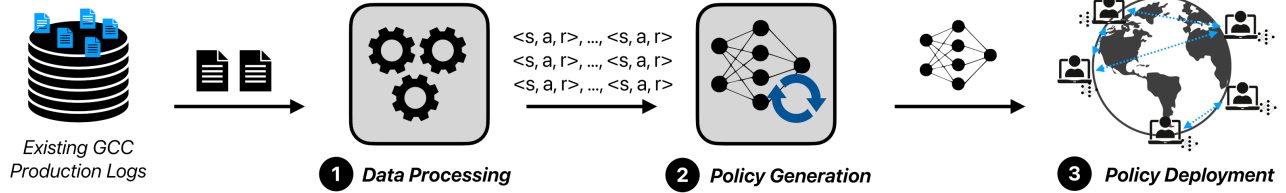


Figure 5: Overview of Tarzan’s 3 phases: (1) data processing for extracting trajectories of (State, Action, Reward) tuples from GCC telemetry logs, (2) policy generation for model training, and (3) policy deployment.

to address the effects of environmental variance can increase P90 video freeze rates over $10\times$. To have an effective solution, we need a way to explicitly express and account for environmental noise.

4 DESIGN

Fig. 5 describes Tarzan’s workflow. First, Tarzan consumes existing production logs or builds on existing logging instrumentation to extract telemetry signals and generate trajectories of (state, action, reward) tuples that reflect the experiences of the underlying rate control algorithm (§4.1). Then, Tarzan leverages these trajectories to train a lightweight neural network for rate control (§4.2). Training occurs entirely offline using only telemetry logs, i.e., no video playback or simulation is required; the resulting policy is then shipped to client devices for deployment (§4.3). We describe implementation details in §4.4.

4.1 Data Collection & Processing

Tarzan operates on production telemetry data that reflects the experiences of in-house rate control algorithms. These logs are typically already captured for other purposes such as debugging, observability, and quality assurance [2, 6]. For example, recently released logs from Microsoft Teams capture periodic (every 60 ms) application and transport layer metrics (e.g., packet loss, packet delay, received bitrate, and target bitrate) along with session-level QoE metrics (e.g., duration of video freezes, average media bitrate received) [2]. If the existing production logs do not provide the necessary data, we can build on existing instrumentation platforms to extract the additional data (e.g., Zoom, Microsoft Teams, WebRTC have built-in logging capabilities [1, 2, 4, 7, 9, 10]). Once logs are aggregated across clients to a central server, we apply Tarzan’s processing logic to extract trajectories of (state, action, reward) tuples.

We define the state vector and action based on prior work [22, 47, 48]. The state vector is a window of periodically captured transport and application-level statistics (we use a window of 1 second). We describe the state vector in Table 1. We find that augmenting the state vector inputs with four additional features further improves performance: the previous bitrate action, the minimum RTT observed so far, the number of timesteps since the last transport feedback report was received, and the number of timesteps since the last packet loss report was received. We measure the impact of

State Vector Inputs
Sent Bitrate
Acknowledged Bitrate
Previous Action
One-Way Packet Delay
One-Way Packet Delay Jitter
Inter-packet Arrival Delay Variation
Round Trip Time
Minimum Round Trip Time Observed So Far
Timesteps since Last Transport Feedback Report
Packet Loss
Timesteps since Last Packet Loss Report

Table 1: State vector of transport and application-layer statistics logged every ~ 50 ms.

these additional features in §5.5. The action is the updated target bitrate that is consumed by the application. We define the reward as a function of the achieved bitrate, the average RTT, and the average packet loss. Inspired by prior work, we leverage the following formulation:

$$R = \alpha \cdot \text{throughput} - \beta \cdot \text{delay} - \gamma \cdot \text{loss} \quad (1)$$

We normalize throughput to the range (0, 6 Mbps) and the delay to (0, 1000 ms); we set α to 2, β to 1, and γ to 1.

4.2 Policy Generation

Next, Tarzan leverages the aggregated and preprocessed logs to generate improved rate control policies. In §3, we described an approach to improve upon GCC by rearranging the actions within a GCC log. In this section, we explain how to realize this approach in practice. First, we describe Tarzan’s use of a lightweight neural network to represent a rate control policy on client devices; we then detail how we overcome the challenges of realizing this approach presented in §3.4.

Leveraging neural networks. To reason about potential actions for a given scenario, we need a way to estimate the expected outcomes for (state, action) pairs. To achieve this, we turn to neural networks that we can train offline (using GCC logs) and subsequently deploy to client devices. In particular, we leverage a state-of-the-art learning algorithm, Soft Actor-Critic (SAC) [25].

SAC consumes the trajectories of (state, action, reward) tuples previously experienced by GCC and trains two com-

plementary functions (both represented by parameterizable neural networks): the actor and the critic. The actor network (π_θ) learns a deterministic policy that maps states to actions; the critic network (Q_ϕ) evaluates the expected long-term reward (return) for a given (state, action) pair. SAC leverages the critic to provide a learning signal (via the Q-value) for the actor, enabling it to improve the policy by following the gradient of expected returns.

Following standard Q-Learning [41] techniques, we train the critic network by minimizing the Mean Squared Bellman Error:

$$\mathbb{E}_{(s_t, a_t, r_t) \sim D} \left[(Q_\phi(s_t, a_t) - (r_t + \gamma \cdot \max_{a'} Q_\phi(s_{t+1}, a')))^2 \right] \quad (2)$$

The actor network is updated by maximizing the Q-value predicted by the critic:

$$\max_{\theta} \mathbb{E}_{s \sim D} [Q_\phi(s, \pi_\theta(s))] \quad (3)$$

We train Q_ϕ and π_θ in tandem, repeatedly iterating through the dataset of (state, action, reward) tuples. The pseudocode in Listing 1 describes the key components of the dual training process: updating the critic, and then updating the actor. Upon convergence (and during inference), we only need to retain π_θ : given state s , return $\pi_\theta(s)$.

Algorithm 1: Soft Actor Critic Algorithm

Input: Corpus of GCC Observations: $D \in \langle S, A, R \rangle$

```

1 repeat until convergence:
2   Randomly sample a batch of transitions,
    $B = \{(s, a, r, s')\}$  from  $D$ 
3   Compute target:
4      $y \leftarrow r + \gamma \cdot Q_\phi(s', \pi_\theta(s'))$ 
5   Update critic function:
6      $\nabla_{\phi} \frac{1}{|B|} \sum_{(s, a, r, s') \in B} (Q_\phi(s, a) - y)^2$ 
7   Update actor network:
8      $\nabla_{\theta} \frac{1}{|B|} \sum_{s \in B} Q_\phi(s, \pi_\theta(s))$ 
9 def update_bitrate(state  $s$ ):
10   $a \leftarrow \pi_\theta(s)$ 
11  return  $a$ ;
```

Further, we prepend the actor and critic networks with a learned embedding over the raw state vector to take advantage of the temporal aspect of the state. Following prior work, the state is a windowed series of metrics—we incorporate a Gated Recurrent Unit (GRU) to extract trends over the window and reduce the raw state to a more condensed vector [19]. Implementation details can be found in §4.4.

Conservative learning. While the rate control policies are now trained offline in the cloud, the challenge of a lack of feedback persists (**Challenge #1**). Learning an improved rate control policy requires learning a strategy that deviates from

the behavior seen in GCC. The greater the deviation, the greater the potential risk of extrapolation error; any errors in extrapolating will compound and drastically harm performance. In this section, we describe how the errors come to be in the context of the actor and critic networks, and then we go on to describe a risk mitigation strategy.

Recall that the learned critic function ultimately guides the decision-making policy (actor) to select actions that optimize for the best behavior. The critic Q_ϕ is responsible for learning a regression to estimate the value of (state, action) pairs observed in the dataset. It is also responsible for learning a regression to estimate the value of (state, action) pairs *not seen* in the dataset. The latter is much harder because it requires extrapolating—that is, using values of observed (state, action) pairs to estimate values for unseen (state, action) pairs. As a result, the regressor is likely to be more error-prone for those unseen regions of the state-action space. This is particularly problematic because the actor is trained to learn actions that maximize the critic function (Equation 3). Any mistakes or erroneous value assignments can lead the actor astray; in particular, the actor becomes biased toward selecting actions that have been erroneously assigned high values. The result is a poor-performing policy, one that can be potentially worse than the data that was used to train it.

To address this, we opt for the following approach: when leveraging the output of the learned critic to teach the actor, trust the estimates more when the regressor is confident (i.e., the estimate is based on (state, action) pairs seen or are close to those observed in the dataset) and trust the estimates less when the regressor is less confident (i.e., the estimate is heavily extrapolated). Recall that in cases where GCC performs poorly, it eventually converges to the near-optimal target rate (§3.3)—these sequences provide a sufficient number of examples to confidently extrapolate about alternate trajectories in areas that GCC needs improvement.

In practice, we can achieve this by penalizing the estimated values for low-confidence regions and elevating those for high-confidence regions. Consequently, when the actor is leveraging the output of the critic, it learns to select actions that maximize the modified estimated value instead (i.e., one that takes into account the accuracy of the estimate) and ultimately, avoid falling into a trap of taking actions with erroneously high estimates due to errors in the learned regressor.

In particular, we leverage a state-of-the-art technique known as Conservative Q-Learning (CQL) [27]. CQL adds a regularizer to the critic’s loss function (Equation 2):

$$\alpha \cdot \mathbb{E}_{s \sim D} \left[\mathbb{E}_{a \sim \pi(a|s)} Q(s, a) - \mathbb{E}_{a \sim D} Q(s, a) \right] \quad (4)$$

The regularizer first guides the critic to learn a lower bound on estimated values for all (state, action) pairs (i.e., a “conservative” estimate); simultaneously, it “pushes up” the values for (state, action) pairs observed in the training dataset. CQL provides an adjustable parameter α to identify the appropriate magnitude of the conservative penalty: too high of a penalty

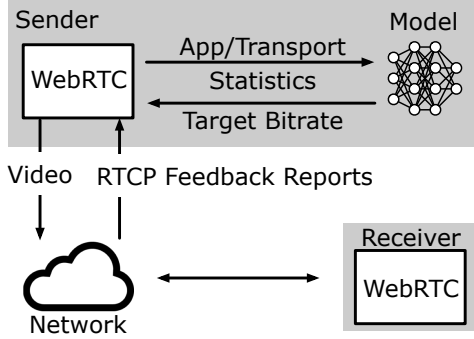


Figure 6: Tarzan deploys its model in the sender application’s rate control logic.

creates a conservative, low-risk policy that performs similarly to the behavior featured in the logs; too low of penalty negates the benefits of this approach altogether, resulting in a risky (and potentially, low-performing) policy. We empirically find that setting $\alpha = 0.01$ achieves the best tradeoff; in our ablation studies in §5.5, we compare different settings of the α parameter.

Distributional representation. The second main challenge of learning from heuristic data collected in production deployment settings is the presence of external phenomena outside the control of the rate control policy that ultimately complicates reasoning about the observed outcomes for a given (state, action) pair (**Challenge #2**). To address this, we opt to explicitly account for the variance in expected return for a given (state, action) pair by modifying the way the learned value is represented. Traditionally, the critic learns a scalar value—i.e., the expected value of starting at state s and taking action a . We modify the critic function to learn a *distribution* over expected outcomes instead [15]. A probability distribution explicitly accounts for the possibility of multiple different futures, despite the bitrate agent taking the same action. Directly encoding a probability distribution into the model provides a richer picture and a more comprehensive way of representing the effects of any given decision.

To implement this, we modify the output of the critic function to be a vector (representing a distribution) instead of a scalar and update the loss function to support a vector representation. In line with prior work, we incorporate the Quantile Huber loss function, which compares distributions and penalizes estimates differently depending on which quantile they belong [20].

4.3 Policy Deployment

Based on findings from our generalization study (§5.3), Tarzan achieves performance wins across diverse network scenarios, provided that their corresponding state/action distributions are represented in the consumed telemetry logs. To adapt to new network environments, Tarzan continuously monitors these logs, and if a shift in the underlying state/action distribution is detected, the system triggers model retraining.

Deploying Tarzan’s learned rate control algorithm requires code changes to the application’s rate control logic and sending over the weights parameterizing the learned model (Fig. 6). Inside the application, we spawn an additional Python process responsible for serving the model. The application code and Python process communicate via an interprocess pipe; the Python process consumes live telemetry data logged by the application instrumentation code and outputs an updated target bitrate.

4.4 Implementation

Inspired by OpenNetLab [21], we implement Tarzan on top of WebRTC [8], a widely used open-source framework for real-time video conferencing applications. In our current implementation, in line with prior work [23], we target unidirectional video without audio. Further, to isolate the effects of rate control in WebRTC, we set `DegradationPreference=DISABLED` [5]. We leverage the PyTorch [33] and d3rlpy [38] Python libraries to train and deploy Tarzan’s learned rate control algorithm. We set the conservative loss penalty hyperparameter (α) to 0.01 and the number of quantiles (N) in our distributional value representation to 32. The actor and critic neural networks have 2 hidden layers of size 256; the GRU has a hidden unit size of 32.

5 EVALUATION

We evaluated Tarzan on a diverse set of networks, both in emulation and in the wild. Our key findings are:

- Tarzan delivers substantial QoE improvements over GCC in emulated networks, increasing average video bitrates by 15–39% while reducing video freeze rates by 60–100%.
- Tarzan achieves performance similar to that of existing (impractical) data-driven approaches using online RL, with average bitrates within 0.5–13.1% and freeze rates within 0–19%.
- Tarzan can achieve wins across diverse network scenarios, provided that they are sufficiently represented in consumed telemetry logs.
- We further deploy and evaluate Tarzan on real cellular networks in four different cities across the U.S. On target networks with high dynamism, Tarzan increases average video bitrates by 17.7% while maintaining similar levels of video freezes.

5.1 Methodology

Experiment setup and testbed. For lack of access to a production video conferencing deployment, we set up our own testbed to collect GCC logs and evaluate Tarzan. We use the AlphaRTC [21] fork of WebRTC to run an end-to-end client-to-client video conferencing workflow. We run both clients on a single machine and use a network emulation tool (Mahimahi [31]) to emulate the network between clients.

To evaluate Tarzan on a diverse and challenging set of networks, we created a corpus of 87 hours of network bandwidth

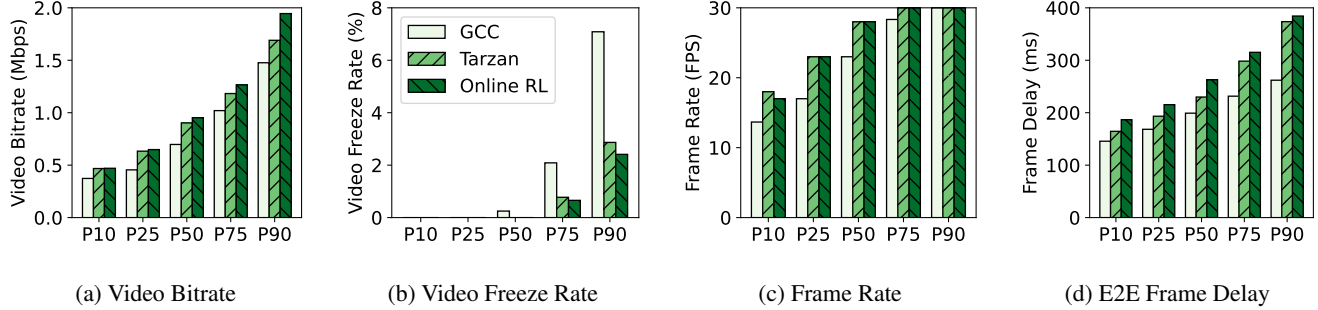


Figure 7: On emulated network traces, Tarzan consistently outperforms GCC and nearly matches the online RL baseline while avoiding QoE degradations during training.

traces from two real-world datasets: FCC [3] broadband traces and Norway [36] cellular traces. We split each trace into 1-minute chunks. Following prior work [29], we filtered out traces with an average bandwidth of <0.2 Mbps or >6 Mbps. We used 60% of the traces for training, 20% for validation, and 20% for testing. Each network trace is randomly assigned to one of the following RTTs: 40, 100, and 160 ms. We use a queue length of 50 packets.

Similar to prior work [37], instead of recording and sending live video, we modify the WebRTC codebase to read from a prerecorded video. We use 9 different one-minute videos from a video conferencing dataset [32]; we randomly assign a video to each bandwidth trace.

To create a corpus of “production logs,” we collect telemetry data from running GCC on the network traces in the training dataset. We note that although production logs from existing video conferencing platforms [2] exist, we do not have access to their systems to perform an evaluation; therefore we opt to use data from our own setup.

QoE metrics. We evaluate QoE across the following metrics: (1) average received *video bitrate* (Mbps), (2) *video freeze rate*—fraction of session experiencing freezes (as defined by WebRTC [13]), (3) *frame rate* (FPS), and (4) average end-to-end *frame delay*. The first three metrics are already available in the WebRTC application logs. To calculate the end-to-end frame delay, we embed a QR code into each video frame to indicate the frame ID. We then calculate the timestamp difference between when the frame is read and when the corresponding frame is displayed. Note that we only measure the end-to-end frame delay for experiments done on emulated networks because on real networks, the clients are located on different devices and require nontrivial time synchronization.

Baseline algorithms. We compare Tarzan against the following baselines:

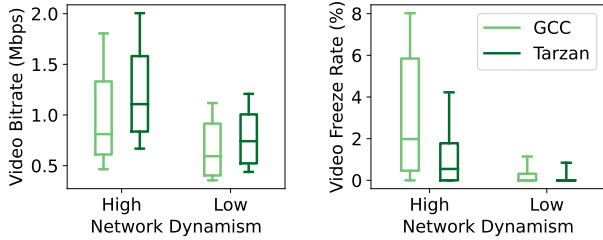
- **Google Congestion Control (GCC)** [17]: the de facto rate control algorithm for video conferencing. It employs hand-tuned rule-based heuristics to characterize network behavior based on recent packet delay and loss measurements. We use the built-in implementation of GCC in WebRTC.

- **Online RL:** an online reinforcement learning-based approach. We implement an in-house solution following the design and methodology of prior work [22, 47, 48]. The details of our implementation are provided in §A.1. Note that the reported results exclude quality degradations incurred during training (see §2.2); instead, we only present results from the model that performs the best on the test dataset.
- **Behavior Cloning (BC)** [34, 42]: an alternative offline learning strategy that trains a rate control policy solely on existing logs, by imitating the behavior featured in the logs through supervised learning.
- **Critic Regularized Regression (CRR)** [40]: another offline learning strategy that relies exclusively on existing logs for training. It is the underlying mechanism for Sage [45], a related work aimed at learning improved TCP congestion control algorithms from logs generated by dozens of different existing CC algorithms. Whereas CQL focuses on conservatively adjusting the critic function to avoid overestimating out-of-distribution actions, CRR regularizes the policy by using the critic’s estimated values to guide the actor toward high-value actions of the dataset.

5.2 Overall Performance

Main results. Fig. 7 compares Tarzan with GCC and Online RL. There are two main takeaways. First, Tarzan consistently improves upon GCC; across reported percentiles, Tarzan increases the average video bitrate by 14.5–39.2%, decreases the video freeze rate by 59.5–100%, and increases the frame rate by 0–35.3%. End-to-end frame delays are within the 400 ms interactivity threshold [11], even with RTTs up to 160 ms. Second, despite learning completely offline, Tarzan’s performance nearly matches that of the online RL baseline. Across percentiles, Tarzan achieves an average video bitrate within 0.5–13.1% of Online RL’s average. Tarzan’s P75 and P90 video freeze rates are 0.77% and 2.87%, respectively, only slightly higher than Online RL’s rates of 0.66% and 2.41%. For comparison, GCC’s P75 and P90 video freeze rates are 2.09% and 7.09%.

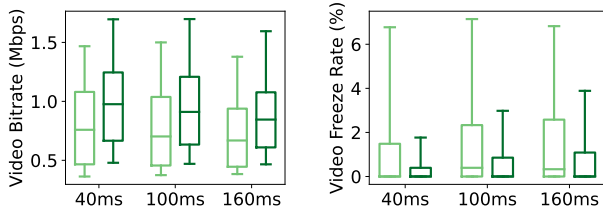
Breakdown by dynamism. To better understand how Tarzan performs in the network conditions where GCC performs



(a) Video Bitrate

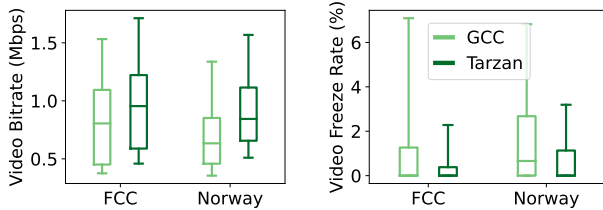
(b) Freeze Rate

Figure 8: Evaluating Tarzan’s performance in network traces of varying network dynamism, measured by the degree of bandwidth variation. Whiskers show P10–P90. Tarzan’s win relative to GCC is higher under high network dynamism.



(a) Video Bitrate (Diff. RTT)

(b) Freeze Rate (Diff. RTT)



(c) Video Bitrate (Diff. Dataset)

(d) Freeze Rate (Diff. Dataset)

Figure 9: Evaluating Tarzan’s performance in network traces of varying delay (RTT) and dataset. Whiskers show P10–P90.

poorly, we split the dataset of network traces based on the degree of network dynamism. Specifically, we calculate the standard deviation of 1-second network bandwidth chunks within each trace and split the dataset along the mean standard deviation across traces. We observe that Tarzan achieves its largest wins over GCC in traces with high bandwidth dynamism – across reported percentiles, Tarzan increases the average video bitrate by 10.8–43.8% and decreases the video freeze rate by 47.4–100% (Fig. 8). In contrast, for traces with less dynamism, Tarzan increases the average video bitrate by 8.0–29.6% and decreases the video freeze rate by 26.2–100%.

Breakdown by network dataset & delay. In Fig. 9, we break down the results from Fig. 7 based on different characterizations of the underlying network traces. We find that as network delay increases, Tarzan’s P50 video bitrate decreases (976 kbps \rightarrow 911 kbps \rightarrow 845 kbps) and its P75 video freeze rates increase (0.39% \rightarrow 0.86% \rightarrow 1.09%). We report P75

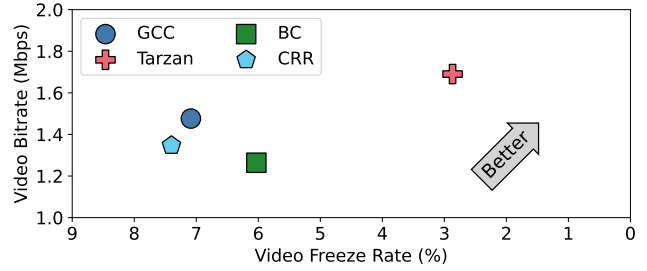
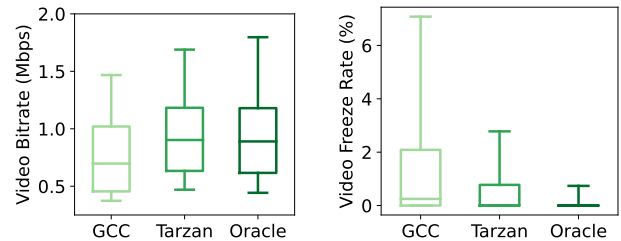


Figure 10: Comparing Tarzan’s P90 performance against additional baselines. Tarzan outperforms all baselines in both bitrate and freezes.



(a) Video Bitrate

(b) Freeze Rate

Figure 11: Comparing Tarzan against an approximate oracle algorithm that represents an upper bound on performance improvements over GCC; whiskers correspond to P10 and P90. Tarzan achieves performance close to the oracle.

video freeze rates because P50 video freeze rates are 0%. This is expected as higher network delays increase the time it takes for a model to receive feedback about potential network congestion and react appropriately; as a result, the model is less aggressive in its bandwidth ramp-ups. When split by dataset, Tarzan performs better in the FCC dataset than in the Norway dataset (954 kbps vs. 844 kbps P50 video bitrates, 0.39% vs. 1.13% P75 video freeze rates). The Norway dataset was collected over 3G cellular networks and therefore, features more network dynamism than the traces in the FCC dataset (which were captured on wired broadband networks).

Additional baselines. In Fig. 10, we compare Tarzan with two alternative learning strategies: Behavior Cloning (BC) and Critic Regularized Regression (CRR). We find that BC behaves less aggressively than Tarzan, achieving a P90 video bitrate that is 14.4% lower than GCC, whereas Tarzan increases the bitrate by 14.5% compared with GCC. This difference arises because BC only aims to imitate the behavior observed in the training logs and fails to effectively extrapolate to unseen scenarios. CRR, the underlying learning algorithm in Sage [45], performs worse than GCC on both metrics, with a 4.4% increase in the P90 video freeze rate and an 8.8% decrease in the P90 video bitrate. We hypothesize that this is due to the lack of state-action coverage featured in the logs of Google Congestion Control; the logs of Sage, on the

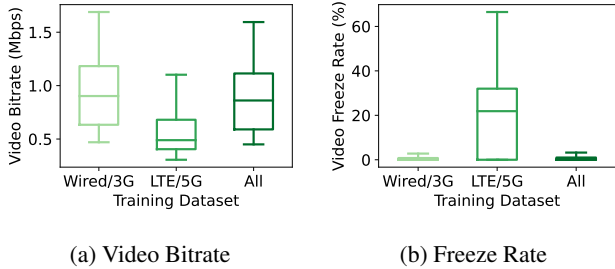


Figure 12: Evaluating Tarzan’s performance on the Wired/3G network dataset when varying the network telemetry dataset consumed; whiskers show P10–P90.

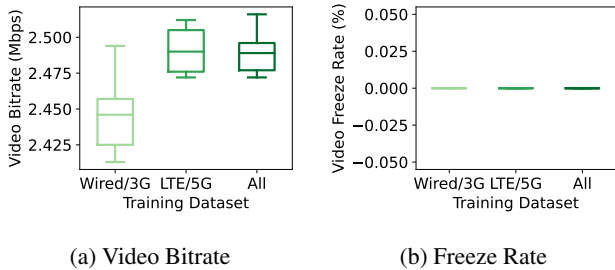


Figure 13: Evaluating Tarzan’s performance on the LTE/5G network dataset when varying the content of the network telemetry dataset consumed; whiskers show P10–P90.

other hand, contain the experience of dozens of different CC algorithms reducing the likelihood of erroneous estimates.

Comparison to approximate oracle. In §3.3, we implemented an approximate oracle algorithm to estimate the maximum possible improvement over GCC. This algorithm serves as an estimate of the (unattainable) upper bound on performance improvements. Fig. 11 compares this oracle with Tarzan. Across reported percentiles, Tarzan comes within 6% of the oracle’s achieved video bitrate. Compared with GCC’s video freeze rates of 2.1% at P75 and 7.1% at P90, Tarzan significantly reduces these rates to 0.8% and 2.9%, while the oracle further lowers them to 0% and 0.7%. These additional reductions are expected since the oracle algorithm has access to ground-truth network bandwidths in advance.

5.3 Generalization & Deployment Considerations

In this section, we explore the limits of Tarzan’s ability to generalize to network conditions and network types not represented in the production telemetry dataset. Further, we seek to quantify the benefits of model specialization to a given set of network conditions. In particular, we consider an additional set of network traces captured on LTE and 5G networks [24]. Following our previous methodology, we collected GCC logs on these LTE/5G traces and trained a policy. We then evaluated this policy on network traces from the main dataset composed of wired and 3G traces. We report the results in Fig. 12. There are two main takeaways.

First, we find Tarzan’s generated policies do not perform

Scenario	Network	Cities
A	4G/LTE	Princeton, NJ; San Jose, CA
B (new cities)	4G/LTE	New York City, NY; Nashville, TN

Table 2: Cities and network types for in-the-wild evaluation.

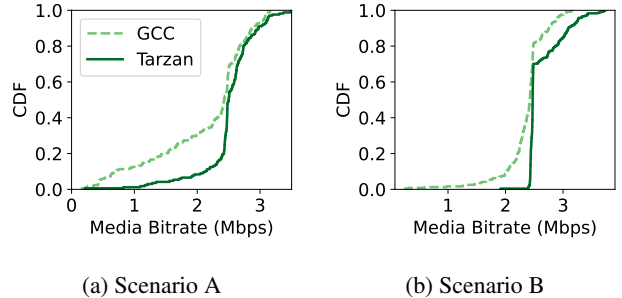


Figure 14: Evaluating Tarzan on real-world cellular networks; scenarios are described in Table 2. Tarzan outperforms GCC across video bitrate percentiles, while video freezes remain statistically indistinguishable between the two (not shown).

well on network dynamics and conditions significantly different from those featured in consumed telemetry logs. For example, the LTE/5G policy performs significantly worse than the Wired/3G policy when evaluated on Wired/3G networks, decreasing the P50 video bitrate by 45.8% and increasing the P75 video freeze rate by 40.3 \times . This is expected due to underlying state/action distribution differences in the corresponding GCC logs (e.g., GCC’s average video bitrate is 1.6 Mbps higher in the LTE/5G dataset).

Second, we observe that despite this, specializing a model for a specific set of network traces is unnecessary; we find that using slightly more general models can perform across network conditions as long as those settings are represented in the consumed telemetry logs. For example, we trained a model on both network datasets and compared it to the model trained on only the Wired/3G dataset. The Wired/3G model achieves slightly higher (4.6%) P50 video bitrates and slightly lower P75 video freeze rates (1.00% \rightarrow 0.77%).

We performed a similar analysis on the LTE/5G dataset, evaluating the aforementioned model on these network traces (Fig. 13). We find that the above trends hold (e.g., the Wired/3G policy decreases median video bitrate by 1.8%).

5.4 Real World Experiments

We evaluated Tarzan and GCC in the wild on cellular networks in 4 different cities throughout the United States (Table 2). In these experiments, we set up conferencing sessions with a client running on a Macbook Pro (tethered to a Google Pixel) and a server in the cloud. Experiments were performed in a collection of mobility scenarios (e.g., train, bus, car, walking, and stationary). To generate a dataset of GCC logs, we collected over 8 hours of video conferencing calls using GCC in City A on a 4G/LTE network. Once Tarzan generated a pol-

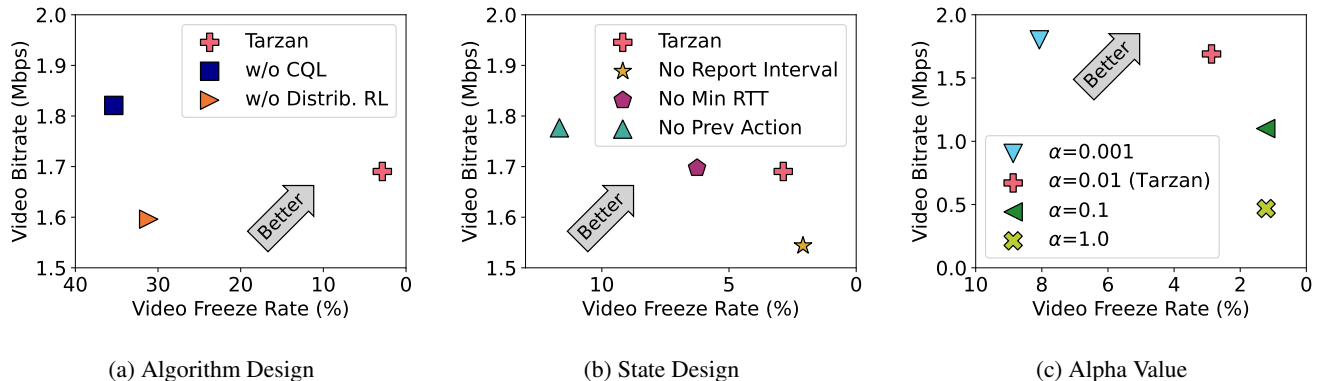


Figure 15: Ablation results, varying the algorithm design, state design, and alpha. Markers correspond to P90. Tarzan’s design achieves the best bitrate-freeze tradeoff.

icity, we evaluated the resulting model in 2 different scenarios: (a) the same network and city and (b) different cities. During our evaluation, we alternated running GCC and the generated policy, collecting over 4 hours of data for each scenario.

We observe that Tarzan’s wins over GCC extend to cellular networks in both scenarios, increasing video bitrates across reported percentiles by $3.0\%–2.1\times$ (Fig. 14a) and $2.0\%–20.8\%$ (Fig. 14b). Video freezes—as a rare event—are inherently challenging to measure reliably [44]. While we currently lack sufficient evidence to draw definitive conclusions, the observed rates across 120 runs per policy/scenario appear statistically indistinguishable (results not shown).

5.5 Ablation Studies and Microbenchmarks

Algorithm design ablation. Fig. 15a compares Tarzan with two variants: (1) Tarzan without the conservative learning regularizer, and (2) Tarzan without the distributional representation. Removing the regularizer, which adjusts the learned estimates of the critic function based on sample confidence, makes the model prone to actions with erroneously high estimated values and results in $11.3\times$ higher P90 video freeze rate. Without the distributional representation, which accounts for external phenomena outside the control of the bitrate decision-making policy, P90 video bitrates drop by 5.6% and P90 video freeze rates increase by $9.9\times$.

Varying state design. Fig. 15b shows the benefits of the additional state features. Removing “Report Intervals”, which indicates the staleness of the sender-side transport feedback report, leads to an 8.7% lower video bitrate. Removing “Min RTT”, which indicates how fast the client can receive (and react to) feedback and helps control the model’s aggression, leads to a $1.2\times$ higher freeze rate. Removing “Prev Action”, which enables smooth rate control, results in a $3.1\times$ increase in the video freeze rate.

CQL α parameter sensitivity. α dictates the relative weight of the conservative penalty in the learning algorithm. In Fig. 15c, a larger α creates a conservative, low-risk policy ($\sim 57\%$ lower freeze rates), but lowers video bitrates by 34.9%

and 72.3% , respectively. In contrast, $\alpha < 0.01$ increases the amount of deviation (and therefore risks: $1.8\times$ higher video freeze rate) albeit increasing bitrate by 6.6% .

System overheads. We study the compute and storage overhead of deploying Tarzan. The compressed (state, action, reward) logs take ~ 117 kB for a 1-minute call. Tarzan’s generated policy (weights) is 316 kB (corresponding to $79k$ parameters) and takes ~ 6 ms to run on the CPU.

6 RELATED WORK

Alternative designs and knobs for video conferencing. Recent work has explored different optimization dimensions in videoconferencing. Salsify [23] co-designs the video codec and transport protocol to quickly respond to changing network conditions and achieve low latency. Gemino [39] designs a neural codec for high perceptual quality in low bandwidth environments. Grace [18] designs a loss-resilient neural codec. AFR [30] adapts the frame rate for video conferencing applications with ultra-high-definition demand. Tarzan is complementary to these works and can be extended to incorporate these alternate dimensions, which we leave for future work.

ML for networked-systems. ML has also been applied to address other problems in networked systems. Pensieve [29] trains an RL agent for adaptive bitrate (ABR) selection in video streaming. Puffer [44] trains an ML-based ABR algorithm in situ, i.e. directly on real-world deployment environments rather than simulators. Unlike video streaming, which uses discrete bitrate adaptation, video conferencing requires continuous rate control, has tighter latency constraints, and performs fine-grained decision-making every 50 ms while encoding and compressing on the fly. Orca [14]’s RL-based congestion control (CC) algorithm generalizes and is performant on different networks. Sage [45] also learns from logs of CC algorithms but requires additional data collection with multiple expert policies. In contrast, Tarzan learns from existing logs of a single policy (e.g., Google Congestion Control).

7 CONCLUSION

In this paper, we presented Tarzan, a system for *practically* learning improved bitrate control algorithms for video conferencing. Whereas existing data-driven reinforcement learning-based approaches fall short of meeting the practicality constraints of production settings, Tarzan demonstrates the possibility of learning from data already collected in existing system telemetry logs (and avoiding the QoE disruptions of prior work) to generate improved bitrate control algorithms.

REFERENCES

- [1] Accessing Zoom Meeting and Phone Statistics. https://support.zoom.com/hc/en/article?id=zm_kb&sysparm_article=KB0070504.
- [2] Bandwidth Estimation Challenge Dataset. <https://www.microsoft.com/en-us/research/academic-program/bandwidth-estimation-challenge/data>.
- [3] Measuring Broadband America. <https://www.fcc.gov/general/measuring-broadband-america>.
- [4] Microsoft Teams Client Diagnostic Logs. <https://learn.microsoft.com/en-us/microsoftteams/log-files>.
- [5] RTP Parameters. https://source.chromium.org/chromium/chromium/src/+main:third_party/webrtc/api/rtp_parameters.h.
- [6] Understanding the Consent Settings in Data & Privacy Center. https://support.zoom.com/hc/en/article?id=zm_kb&sysparm_article=KB0057779.
- [7] Use real-time telemetry to troubleshoot poor meeting quality. <https://learn.microsoft.com/en-us/microsoftteams/use-real-time-telemetry-to-troubleshoot-poor-meeting-quality>.
- [8] WebRTC. <https://webrtc.org/>.
- [9] WebRTC Logging. <https://webrtc.github.io/webrtc-org/native-code/logging/>.
- [10] Zoom Service Quality Logging. <https://developers.zoom.us/docs/video-sdk/web/quality/>.
- [11] G.114 One-way transmission time. Technical report, International Telecommunication Union, May 2003.
- [12] Closing the Simulation-to-Reality Gap for Deep Robotic Learning, 2017. <https://research.google/blog/closing-the-simulation-to-reality-gap-for-deep-robotic-learning/>.
- [13] Identifiers for WebRTC’s Statistics API, July 2018. <https://www.w3.org/TR/webrtc-stats/>.
- [14] S. Abbasloo, C.-Y. Yen, and H. J. Chao. Classic Meets Modern: a Pragmatic Learning-Based Congestion Control for the Internet. In *Proceedings of the Annual conference of the ACM Special Interest Group on Data Communication on the applications, technologies, architectures, and protocols for computer communication*, pages 632–647, 2020.
- [15] M. G. Bellemare, W. Dabney, and M. Rowland. *Distributional Reinforcement Learning*. MIT Press, 2023.
- [16] K. Bousmalis, A. Irpan, P. Wohlhart, Y. Bai, M. Kelcey, M. Kalakrishnan, L. Downs, J. Ibarz, P. Pastor, K. Konolige, S. Levine, and V. Vanhoucke. Using Simulation and Domain Adaptation to Improve Efficiency of Deep Robotic Grasping. In *2018 IEEE International Conference on Robotics and Automation (ICRA)*, page 4243–4250. IEEE Press, 2018.
- [17] G. Carlucci, L. De Cicco, S. Holmer, and S. Mascolo. Analysis and Design of the Google Congestion Control for Web Real-time Communication (WebRTC). In *Proceedings of the 7th International Conference on Multimedia Systems*, pages 1–12, 2016.
- [18] Y. Cheng, Z. Zhang, H. Li, A. Arapin, Y. Zhang, Q. Zhang, Y. Liu, K. Du, X. Zhang, F. Y. Yan, et al. Grace: Loss-resilient real-time video through neural codecs. In *21st USENIX Symposium on Networked Systems Design and Implementation (NSDI ’24)*, pages 509–531, 2024.
- [19] K. Cho, B. van Merriënboer, Ç. Gülçehre, F. Bougares, H. Schwenk, and Y. Bengio. Learning Phrase Representations using RNN Encoder-Decoder for Statistical Machine Translation. *CoRR*, abs/1406.1078, 2014.
- [20] W. Dabney, M. Rowland, M. Bellemare, and R. Munos. Distributional Reinforcement Learning with Quantile Regression. In *Proceedings of the AAAI Conference on Artificial Intelligence*, volume 32, 2018.
- [21] J. Eo, Z. Niu, W. Cheng, F. Y. Yan, R. Gao, J. Kardhashi, S. Inglis, M. Revow, B.-G. Chun, P. Cheng, et al. OpenNetLab: Open platform for RL-based Congestion Control for Real-Time Communications. *Proc. of AP-Net*, 2022.
- [22] J. Fang, M. Ellis, B. Li, S. Liu, Y. Hosseinkashi, M. Revow, A. Sadvnikov, Z. Liu, P. Cheng, S. Ashok, et al. Reinforcement Learning for Bandwidth Estimation and Congestion Control in Real-Time Communications. *arXiv preprint arXiv:1912.02222*, 2019.
- [23] S. Fouladi, J. Emmons, E. Orbay, C. Wu, R. S. Wahby, and K. Winstein. Salsify: Low-Latency Network Video through Tighter Integration between a Video Codec and a Transport Protocol. In *15th USENIX Symposium on Networked Systems Design and Implementation (NSDI ’18)*, pages 267–282, 2018.
- [24] M. Ghoshal, Z. J. Kong, Q. Xu, Z. Lu, S. Aggarwal, I. Khan, Y. Li, Y. C. Hu, and D. Koutsonikolas. An In-Depth Study of Uplink Performance of 5G mmWave Networks. In *Proceedings of the ACM SIGCOMM Workshop on 5G and Beyond Network Measurements, Modeling, and Use Cases*, pages 29–35, 2022.
- [25] T. Haarnoja, A. Zhou, P. Abbeel, and S. Levine. Soft Actor-Critic: Off-Policy Maximum Entropy Deep Reinforcement Learning with a Stochastic Actor. In *International conference on machine learning*, pages 1861–1870. PMLR, 2018.
- [26] A. Hussein, M. M. Gaber, E. Elyan, and C. Jayne. Imi-

- tation Learning: A Survey of Learning Methods. *ACM Computing Surveys (CSUR)*, 50(2):1–35, 2017.
- [27] A. Kumar, A. Zhou, G. Tucker, and S. Levine. Conservative Q-Learning for Offline Reinforcement Learning. *Advances in Neural Information Processing Systems*, 33:1179–1191, 2020.
- [28] S. Levine, A. Kumar, G. Tucker, and J. Fu. Offline Reinforcement Learning: Tutorial, Review, and Perspectives on Open Problems. *arXiv preprint arXiv:2005.01643*, 2020.
- [29] H. Mao, R. Netravali, and M. Alizadeh. Neural Adaptive Video Streaming with Pensieve. In *Proceedings of the conference of the ACM special interest group on data communication*, pages 197–210, 2017.
- [30] Z. Meng, T. Wang, Y. Shen, B. Wang, M. Xu, R. Han, H. Liu, V. Arun, H. Hu, and X. Wei. Enabling High Quality Real-Time Communications with Adaptive Frame-Rate. In *20th USENIX Symposium on Networked Systems Design and Implementation (NSDI '23)*, pages 1429–1450, 2023.
- [31] R. Netravali, A. Sivaraman, S. Das, A. Goyal, K. Winstein, J. Mickens, and H. Balakrishnan. Mahimahi: Accurate Record-and-Replay for HTTP. In *2015 USENIX Annual Technical Conference (USENIX ATC '15)*, pages 417–429, 2015.
- [32] E. Nowroozi, A. Dehghantanha, R. M. Parizi, and K.-K. R. Choo. A Survey of Machine Learning Techniques in Adversarial Image Forensics. *Computers & Security*, page 102092, 2020.
- [33] A. Paszke, S. Gross, F. Massa, A. Lerer, J. Bradbury, G. Chanan, T. Killeen, Z. Lin, N. Gimelshein, L. Antiga, et al. Pytorch: An imperative style, high-performance deep learning library. *Advances in neural information processing systems*, 32, 2019.
- [34] D. A. Pomerleau. Alvin: An autonomous land vehicle in a neural network. *Advances in neural information processing systems*, 1, 1988.
- [35] A. Raffin, A. Hill, A. Gleave, A. Kanervisto, M. Ernestus, and N. Dormann. Stable-Baselines3: Reliable Reinforcement Learning Implementations. *The Journal of Machine Learning Research*, 22(1):12348–12355, 2021.
- [36] H. Riiser, P. Vigmstad, C. Griwodz, and P. Halvorsen. Commute path bandwidth traces from 3G networks: analysis and applications. In *Proceedings of the 4th ACM Multimedia Systems Conference*, pages 114–118, 2013.
- [37] M. Rudow, F. Y. Yan, A. Kumar, G. Ananthanarayanan, M. Ellis, and K. Rashmi. Tambur: Efficient loss recovery for videoconferencing via streaming codes. In *20th USENIX Symposium on Networked Systems Design and Implementation (NSDI '23)*, pages 953–971, 2023.
- [38] T. Seno and M. Imai. d3rlpy: An offline deep reinforcement learning library. *The Journal of Machine Learning Research*, 23(1):14205–14224, 2022.
- [39] V. Sivaraman, P. Karimi, V. Venkatapathy, M. Khani, S. Fouladi, M. Alizadeh, F. Durand, and V. Sze. Gemino: Practical and Robust Neural Compression for Video Conferencing. In *21st USENIX Symposium on Networked Systems Design and Implementation (NSDI '24)*, pages 569–590, 2024.
- [40] Z. Wang, A. Novikov, K. Zolna, J. S. Merel, J. T. Springenberg, S. E. Reed, B. Shahriari, N. Siegel, C. Gulcehre, N. Heess, and N. de Freitas. Critic Regularized Regression. In *Advances in Neural Information Processing Systems*, volume 33, pages 7768–7778, 2020.
- [41] C. J. Watkins and P. Dayan. Q-learning. *Machine learning*, 8:279–292, 1992.
- [42] B. Widrow. Pattern recognition and adaptive control. *IEEE Transactions on Applications and Industry*, 83(74):269–277, 1964.
- [43] K. Winstein, A. Sivaraman, and H. Balakrishnan. Stochastic forecasts achieve high throughput and low delay over cellular networks. In *10th USENIX Symposium on Networked Systems Design and Implementation (NSDI '13)*, pages 459–471, 2013.
- [44] F. Y. Yan, H. Ayers, C. Zhu, S. Fouladi, J. Hong, K. Zhang, P. Levis, and K. Winstein. Learning in Situ: a Randomized Experiment in Video Streaming. In *17th USENIX Symposium on Networked Systems Design and Implementation (NSDI '20)*, pages 495–511, 2020.
- [45] C.-Y. Yen, S. Abbasloo, and H. J. Chao. Computers Can Learn from the Heuristic Designs and Master Internet Congestion Control. In *Proceedings of the ACM SIGCOMM 2023 Conference*, pages 255–274, 2023.
- [46] Y. Zaki, T. Pötsch, J. Chen, L. Subramanian, and C. Görg. Adaptive congestion control for unpredictable cellular networks. In *Proceedings of the 2015 ACM Conference on Special Interest Group on Data Communication*, pages 509–522, 2015.
- [47] H. Zhang, A. Zhou, Y. Hu, C. Li, G. Wang, X. Zhang, H. Ma, L. Wu, A. Chen, and C. Wu. Loki: Improving Long Tail Performance of Learning-Based Real-Time Video Adaptation by Fusing Rule-Based Models. In *Proceedings of the 27th Annual International Conference on Mobile Computing and Networking*, pages 775–788, 2021.
- [48] H. Zhang, A. Zhou, J. Lu, R. Ma, Y. Hu, C. Li, X. Zhang, H. Ma, and X. Chen. OnRL: Improving Mobile Video Telephony Via Online Reinforcement Learning. In *Proceedings of the 26th Annual International Conference on Mobile Computing and Networking*, pages 1–14, 2020.
- [49] A. Zhou, H. Zhang, G. Su, L. Wu, R. Ma, Z. Meng, X. Zhang, X. Xie, H. Ma, and X. Chen. Learning to Coordinate Video Codec with Transport Protocol for Mobile Video Telephony. In *The 25th Annual International Conference on Mobile Computing and Networking*, pages 1–16, 2019.

Hyperparameter	Value
Learning Rate	5e-5
Batch Size	512
Gradient Steps	500
Replay Buffer Size	1e6
Init. Entropy Coefficient	0.5
GRU Hidden Size	32
Num Parallel Workers	30
Optimizer	Adam

Table 3: Online RL Hyperparameter Values. For all other unspecified hyperparameters, we use the default values of the implementation in Stable Baselines3 [35]. The same learning rate is used for all networks (Q-Values, Actor, and Value function).

A APPENDIX

A.1 Online RL Setup

Experiment Setup and Testbed. Similar to prior work [14, 47], our online RL baseline relies on a cloud server to support the training. The centralized server has an AMD EPYC 7543P 32-core CPU, 256 GB of RAM, and an NVIDIA RTX A6000-48G GPU. We use 30 nodes (“workers”) to emulate end users in our experiments, each with an Intel Xeon D-1548 8-core CPU and 64 GB of RAM. We modify Stable Baselines3 v2.1.0 [35] to support ingesting state-action-reward tuples from parsed traces and use PyTorch v2.0.1 to train and serve the neural network. Similar to prior work, we use a state-of-the-art off-policy algorithm [25]. Following OnRL [48], we implement a fallback mechanism that allows the sender

to temporarily downgrade to the default heuristic (GCC) if catastrophic QoE degradations are detected during training.

In every round of online RL training, the RL server dispatches the latest model to all 30 worker nodes. Similar to how we collect GCC logs in our main experiments, we run both the sender and receiver client on the same node. Each worker uses Mahimahi [31] to replay a random one-minute network bandwidth trace from the same diverse dataset Tarzan uses. At the end of every video conferencing session, each node parses the sender/receiver logs to construct a state-action-reward trace and sends it back to the RL server. The RL server performs one training epoch based on the aggregated state-action-reward tuples across all workers and repeats this process. We enumerate the hyperparameters used by our online RL baseline in Tab. 3.

We retain the state and action formulation as defined in the main text. However, we observe that using the following reward definition for training the online RL policy further improves performance:

$$\begin{aligned}
 R = & throughput \cdot delay \cdot (1 - \gamma \cdot loss) \\
 & - \zeta \cdot \max(prev_action - sending_bitrate, 0) \\
 & - use_gcc \cdot gcc_penalty
 \end{aligned} \tag{5}$$

where $\gamma = 2$, and $\zeta = 3$. *use_gcc* acts as an indicator variable for whether the fallback mechanism was invoked; we set *gcc_penalty* = 0.05. We normalize *throughput*, *delay*, *loss*, *prev_action*, and *sending_bitrate* to (0, 4.5 Mbps), (0, 1000 ms), (0, 1), (0, 4.5 Mbps), and (0, 4.5 Mbps).